Supplementary material (ESI) for Journal of Materials Chemistry
This journal is © The Royal Society of Chemistry 2008

Supplementary Information

for

Novel Catalysts for Low-Temperature Combustion of Diesel Particulate Matter

Nobuhito Imanaka*, Toshiyuki Masui, Takamasa Egawa, and Hayato Imadzu

Department of Applied Chemistry, Faculty of Engineering, Osaka University
2-1 Yamadaoka, Suita, Osaka 565-0871, Japan

*Corresponding author, e-mail: imanaka@chem.eng.osaka-u.ac.jp

Experimental procedures

The CeO_2–Pr_6O_{11}–Bi_2O_3 solid solutions were prepared by a cation complexing method using citric acid. A stoichiometric mixture of 1 mol L^{-1} $Ce(NO_3)_3$, 1 mol L^{-1} $Pr(NO_3)_3$, and 0.5 mol L^{-1} $Bi(NO_3)_3$ aqueous solutions were added to a 1 mol L^{-1} citric acid solution. The total metal cation to citrate ligand ratio was 1:2.1. After stirring at 80 °C for 5 h, the solvent was evaporated at 80 °C using a rotary evaporator. The resulting solid was dried at 80 °C overnight, and the sample was then calcined at 750 °C for 1 h. Before characterization, the samples were gently ground in an agate mortar. In addition, polyvinylpyrrolidone (PVP) was added to the starting solution of some catalysts to enhance the surface area. The molar quantity of PVP was 15 times as high as that of citric acid, or 31.5 times that of the total metal cation.

The catalysts were characterized by X-ray powder diffraction (Rigaku Multiflex). The sample composition was analyzed using an X-ray fluorescence spectrometer (Rigaku ZSX-100e). The textural characteristics were measured by the BET method using nitrogen adsorption at 77 K with a Micromeritics Tristar 3000 adsorption analyzer.

The oxidation activity of soot was tested by running thermogravimetric analysis (TGA) curves (Shimadzu DTG-60H) in air at a heating rate of 2 °C min^{-1}. Each catalyst was mixed with 2 wt% carbon black (Cabot Elftex$^{@}$ 125) and ground in an agate mortar for 5 min to obtain tight contact mixtures. The amount of the reaction mixture (soot + oxide) and air flow rate in the catalytic assays run on the thermo-balance are 30 mg and 20 mL min^{-1}, respectively. The initial temperature (T_i) was determined from the intercept of a linear fit to the observed weight decrease with the zero line in the corresponding TGA curve, and the completion temperature (T_c) was defined as the temperature of 100% soot conversion. A temperature at 50% weight loss (T_{50}) was also determined. In addition, the TGA curves were measured for the most active catalyst using particulate matter supplied by Isuzu Motors. The particulate matter was collected in a diesel filter in the exhaust pipe after carrying out an engine performance test for a five-thousand-cubic-centimetre displacement car with a turboengine.

Temperature programmed reduction (TPR) was carried out for the most active catalyst. The reduction behaviour was examined under a flow of pure H_2 (80 mL min^{-1}) at a heating rate of 5 °C min^{-1} using the thermal conductivity detector of a gas-chromatography instrument (Shimadzu GC-8A). Following the TPR measurements, the total OSC was measured by using a pulse-injection method at 427 °C (700 K). The OSC was determined using a thermal-conductivity detector by comparing the TCD signals obtained with and without the catalyst. Dynamic OSC measurements were also performed by increasing the temperature in a stepwise manner. During the isothermal steps between 200 and 500 °C, alternating pulses of H_2 (0.2 mL) and O_2 (0.2 mL) were injected over the sample at 7 min intervals (maintained under a 100 mL min^{-1} flow of He).

This journal is © The Royal Society of Chemistry 2008

BET surface area, cubic cell parameter, and soot oxidation temperature of the catalysts.

Table S1. BET surface area, cubic cell parameter, and soot oxidation temperature (T_i, T_{50}, and T_c) of the catalysts

Catalyst	PVP addition	BET surface area ($m^2\ g^{-1}$)	Lattice parameter (nm)	Temperature (°C)		
				T_i	T_{50}	T_c
$Ce_{0.63}Pr_{0.16}Bi_{0.21}O_{1.868}$	No	11.6	0.5427	314	375	425
$Ce_{0.54}Pr_{0.24}Bi_{0.22}O_{1.850}$	No	10.0	0.5432	299	372	420
$Ce_{0.48}Pr_{0.30}Bi_{0.22}O_{1.840}$	No	6.7	0.5438	290	376	430
$Ce_{0.39}Pr_{0.39}Bi_{0.22}O_{1.825}$	No	6.3	0.5441	295	394	430
$Ce_{0.24}Pr_{0.54}Bi_{0.22}O_{1.800}$	No	5.8	0.5461	295	388	425
$Ce_{0.54}Pr_{0.14}Bi_{0.32}O_{1.817}$	No	2.5	0.5436	317	374	410
$Ce_{0.55}Pr_{0.14}Bi_{0.31}O_{1.822}$	Yes	17.9	0.5441	291	352	395
$Ce_{0.47}Pr_{0.21}Bi_{0.32}O_{1.805}$	No	4.6	0.5446	287	358	405
$Ce_{0.47}Pr_{0.21}Bi_{0.32}O_{1.805}$	Yes	20.7	0.5448	285	349	389
$Ce_{0.42}Pr_{0.27}Bi_{0.30}O_{1.800}$	No	5.6	0.5464	294	372	418
$Ce_{0.41}Pr_{0.27}Bi_{0.32}O_{1.795}$	Yes	16.9	0.5458	307	360	407
$Ce_{0.35}Pr_{0.32}Bi_{0.33}O_{1.782}$	No	2.7	0.5466	285	375	420
$Ce_{0.33}Pr_{0.33}Bi_{0.34}O_{1.775}$	Yes	20.4	0.5468	313	363	408
$Ce_{0.20}Pr_{0.48}Bi_{0.32}O_{1.760}$	No	6.3	0.5489	285	393	435
$Ce_{0.21}Pr_{0.47}Bi_{0.32}O_{1.762}$	Yes	24.7	0.5484	321	364	415
$Ce_{0.46}Pr_{0.12}Bi_{0.42}O_{1.770}$	No	1.4	0.5460	317	381	420
$Ce_{0.44}Pr_{0.16}Bi_{0.40}O_{1.773}$	No	2.4	0.5465	302	370	410
$Ce_{0.34}Pr_{0.22}Bi_{0.44}O_{1.743}$	No	2.0	0.5479	289	378	424
$Ce_{0.28}Pr_{0.28}Bi_{0.44}O_{1.733}$	No	2.6	0.5490	295	388	425
$Ce_{0.17}Pr_{0.40}Bi_{0.43}O_{1.718}$	No	3.1	0.5514	313	389	430
Carbon black only	----	----	----	458	596	615
CeO_2	No	3.2	0.5410	357	470	555
$Ce_{0.84}Zr_{0.16}O_2$	No	3.1	0.5402	410	480	543
$Ce_{0.68}Zr_{0.17}Bi_{0.15}O_{1.925}$	No	1.7	0.5379	357	423	470
$Ce_{0.64}Zr_{0.16}Bi_{0.20}O_{1.90}$	No	10.8	0.5373	330	407	460

This journal is © The Royal Society of Chemistry 2008

X-ray powder diffraction of the catalysts

X-ray powder diffraction (XRD) patterns of the $Ce_{1-x}Pr_xBi_yO_{2-\delta}$ catalysts are shown in Fig. S1. The catalysts displayed diffraction peaks that were attributable to a cubic fluorite-type structure. Formation of impurity phases was not detected in either sample. The cubic lattice parameter of the catalysts calculated for (3 1 1) diffraction is summarized in Table S1. When the bismuth content is fixed, the diffraction peaks shift to lower angles with increasing praseodymium, and the cubic cell parameter calculated for (3 1 1) diffraction increases slightly (cf. Table S1). This can be explained by an increase in the ionic radius when a praseodymium ion substitutes for a cerium ion. The ionic radius of Pr^{3+} (0.1126 nm)[S1] is larger than that of Ce^{4+} (0.097 nm),[S1] while the ionic radius of Pr^{4+} (0.096 nm)[S1] is a little smaller than that of Ce^{4+}. However, there is no significant increase in the lattice parameter value while increasing Pr-content in Table S1. This suggests that most of Pr is likely to be in 4+ oxidation state in the samples. On the other hand, when the Ce:Pr ratio is constant, the diffraction peaks again shift to lower angles with increasing bismuth content, because the ionic radius of Bi^{3+} (0.117 nm)[S1] is larger than those of Ce^{4+} (0.097 nm)[S1] and Pr^{3+} (0.1126 nm).[S1] Accordingly, the lattice constant of the cubic cell is proportional to the bismuth content. These results demonstrate that both praseodymium and bismuth ions dissolve into the fluorite lattice to form solid solutions.

S1. Shannon, R.D. *Acta Cryst.* **1976**, *A32*, 751–767.

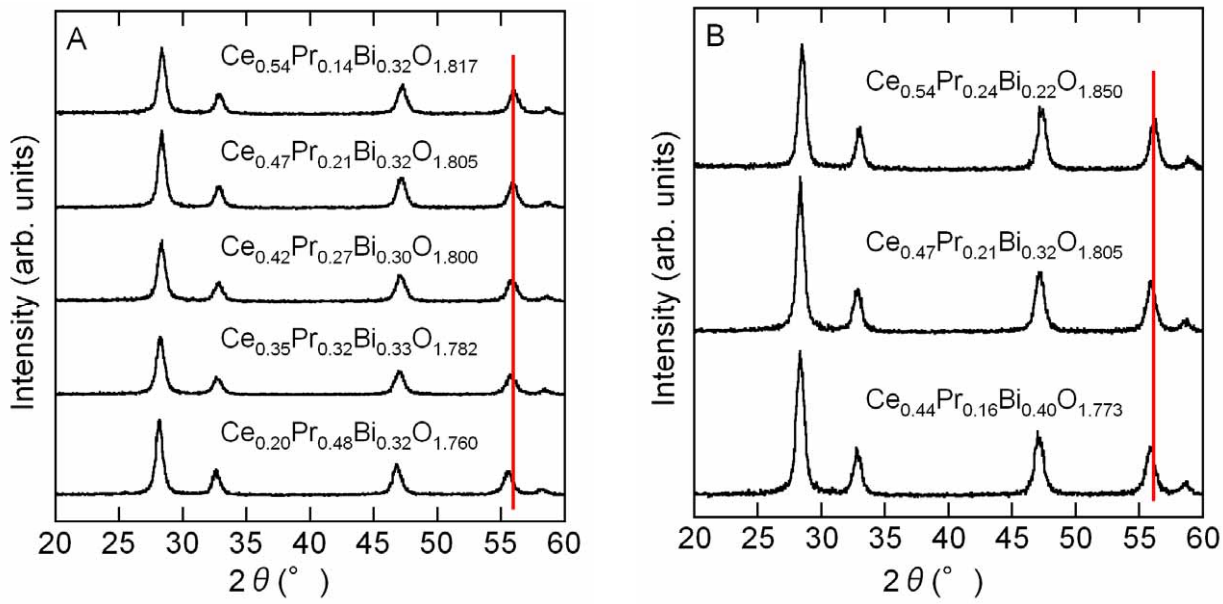

Figure S1. X-ray powder diffraction patterns of CeO_2–Pr_6O_{11}–Bi_2O_3 catalysts. A single phase based on a cubic fluorite structure was observed for all catalysts. The diffraction peaks shift to lower angles with increasing (A) praseodymium or (B) bismuth content, indicating the formation of solid solutions.

This journal is © The Royal Society of Chemistry 2008

Transmission electron microscope (TEM) images of the catalysts

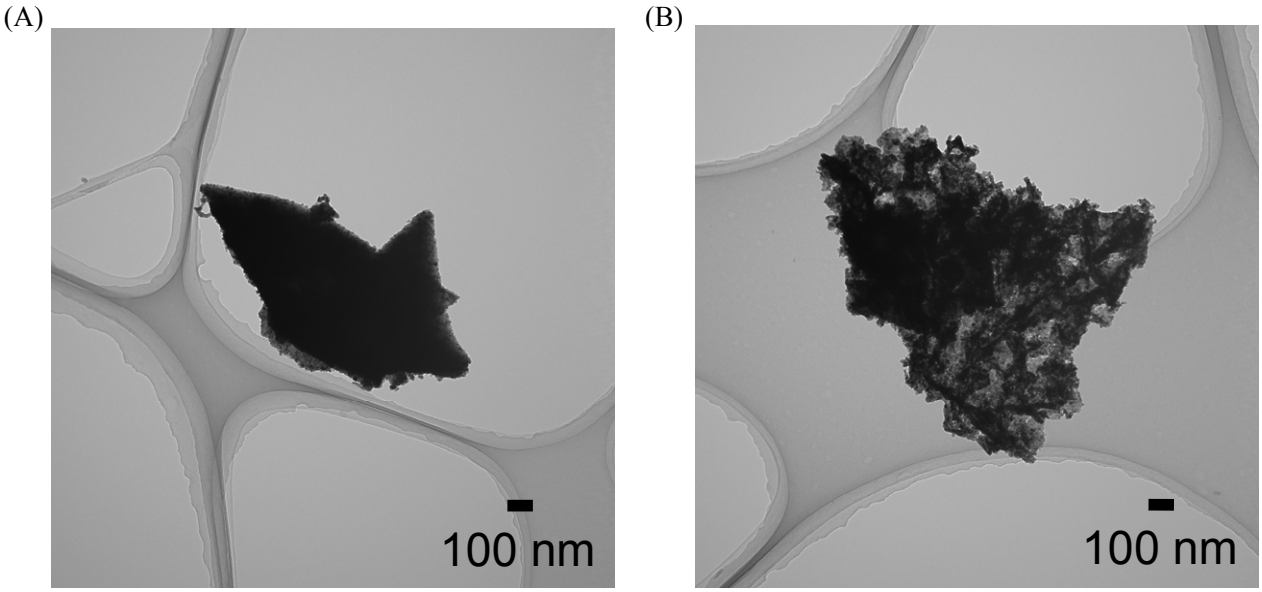

Figure S2. Transmission electron micrographs of the $Ce_{0.47}Pr_{0.21}Bi_{0.32}O_{1.805}$ catalysts. (A) $Ce_{0.47}Pr_{0.21}Bi_{0.32}O_{1.805}$ (CPB) and (B) high-surface-area $Ce_{0.47}Pr_{0.21}Bi_{0.32}O_{1.805}$ prepared using PVP (CPB-PVP).

This journal is © The Royal Society of Chemistry 2008

Evaluation of the activity in the repeated use of the catalyst

The catalytic activities after 5 and 10 times repetition of the soot oxidation up to 750 °C were also tested for the high-surface-area $Ce_{0.47}Pr_{0.21}Bi_{0.32}O_{1.805}$ catalyst prepared using PVP (CPB-PVP) to evaluate the durability of the catalyst. As depicted in Fig. S3 and Table 2, the high oxidation activities were reproducibly observed.

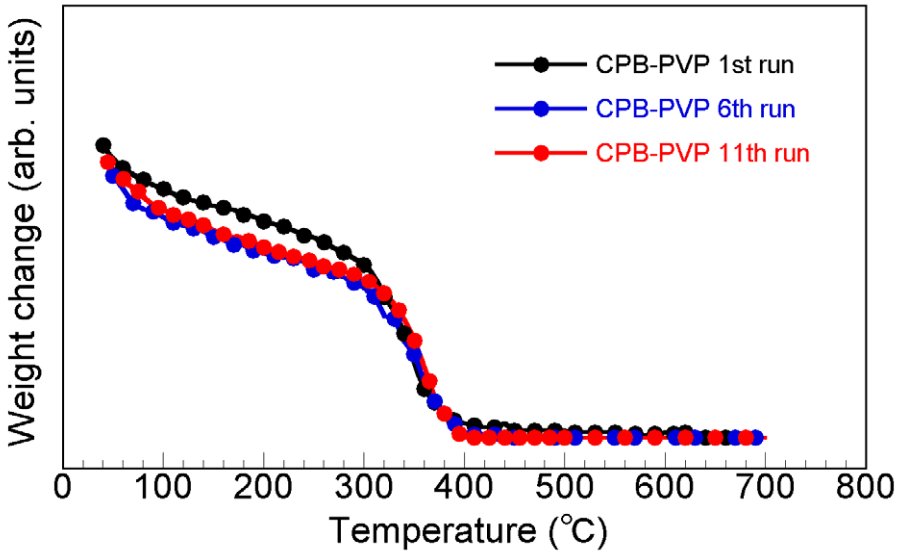

Figure S3. TGA curves for the oxidation of carbon black catalyzed by high-surface-area $Ce_{0.47}Pr_{0.21}Bi_{0.32}O_{1.805}$ prepared using PVP (CPB-PVP) for as-prepared sample (black), aged samples after 5 (blue) and 10 cycles (red) of the carbon black oxidation up to 750 °C.

Table S2. Soot oxidation temperature (T_i, T_{50}, and T_c) of the high-surface-area $Ce_{0.47}Pr_{0.21}Bi_{0.32}O_{1.805}$ prepared using PVP (CPB-PVP) catalysts.

$Ce_{0.47}Pr_{0.21}Bi_{0.32}O_{1.805}$ (CPB-PVP) Catalyst	Temperature (°C)		
	T_i	T_{50}	T_c
1st run (as prepared)	285	349	389
6th run (after 5 cycles)	300	354	391
11th run (after 10 cycles)	308	355	390